Allocation of Hourly Reserve Versus Demand Response for Security-Constrained Scheduling of Stochastic Wind Energy

Cem Sahin, *Member, IEEE*, Mohammad Shahidehpour, *Fellow, IEEE*, and Ismet Erkmen

Abstract—**This paper presents a stochastic method for the hourly scheduling of optimal reserves when the hourly forecast errors of wind energy and load are considered. The approach utilizes the stochastic security-constrained unit commitment (SCUC) model and a two-stage stochastic programming for the day-ahead scheduling of wind energy and conventional units with $N-1$ contingencies. The effect of aggregated hourly demand (DR) response is considered as a means of mitigating transmission violations when uncertainties are considered. The proposed mixed-integer programming (MIP) model applies the Monte Carlo method for representing the hourly wind energy and system load forecast errors. A 6-bus, 118-bus, and the Northwest region of Turkish electric power network are considered to demonstrate the effectiveness of the proposed day-ahead stochastic scheduling method in power systems.**

Index Terms—**Demand response, hourly reserves, load and wind forecast errors, random contingencies, stochastic security-constrained unit commitment (SCUC), wind energy.**

NOMENCLATURE

Indices:

d	Index of load.
i	Index of nonwind energy generating units.
r	Index of DRPs.
s	Index of scenarios.
t	Index of time period (hour).
k	Index of DR provider bid segments.
w	Index of wind energy units.

Dimensions:

NC	Number of $N-1$ contingencies.
ND	Number of system loads.
NDR	Number of DRPs.
NG	Number of nonwind generating units.
NS	Total number of scenarios including contingencies and wind, load forecast error scenarios.
NT	Number of hours.
NQ_r	Number of bidding segments.
NW	Number of wind energy units.

Constraints:

C_{net}	Generalized network constraints in base case and wind, load scenarios.

Variables:

$C_{\mathrm{DRR},r}$	Cost of scheduling DRR by DRP r.
$C_{\mathrm{EDRR},r}$	Cost of utilizing scheduled DRR by DRP r.
DRR_{rt}	Scheduled DR by DRP r at time t.
DRR_{rts}	Deployed DR by DRP r at time t in scenario s.
$F_{c,i}$	Bid-based energy cost function of unit i.
$F_{RR,i}$	Bid-based cost function of unit i regulation reserve.
$F_{SR,i}$	Bid-based cost function of unit i spinning reserve.
I	Commitment state.
P	Power generation.
P_{IMB}	Power generation in regulation interval.
$P_{\Psi,wts}$	Wind generation of unit w at time t and scenario s.
$P_{\mathrm{curt},wts}$	Curtailed wind generation of unit w at time t and scenario s.
RR	Regulation reserve.
RR_d	Scheduled regulation-down reserve.
RR_{its}	Deployed regulation reserve of unit i at time t in scenario s.
RR_u	Scheduled regulation-up reserve.
SR	Deployed spinning reserve.
SR_d	Scheduled spinning-down reserve.
SR_{its}	Deployed spinning reserve by unit i at time t in scenario s.
SR_u	Scheduled spinning-up reserve.
SD	Shutdown cost.

Manuscript received October 31, 2011; revised June 06, 2012; accepted July 28, 2012. Date of publication September 28, 2012; date of current version December 12, 2012.

C. Sahin and I. Erkmen are with the ECE Department, Middle East Technical University, Ankara 6800, Turkey (e-mail: cem.sahin@uzay.tubitak.gov.tr; erkmen@metu.edu.tr).

M. Shahidehpour is with the ECE Department, Illinois Institute of Technology, IL Chicago, IL 60616-3793 USA (e-mail: ms@iit.edu).

Digital Object Identifier 10.1109/TSTE.2012.2213849

SU	Startup cost.
u_{rts}^{k}	Binary variable (1 if point k of offer package DRP r at time t in scenario s is utilized, 0 otherwise).
U_{rt}^{k}	Binary variable (takes the value 1 if point k of offer package DRP r at time t is scheduled, 0 otherwise).
y_{it}	Startup indicator (1 if unit i is started up at time t).
z_{it}	Shut down indicator (1 if unit i is shut down at time t).
ψ_{wts}	Speed of wind energy unit w at hour t in scenario s.

Constants:

A_{w}	Area swept by the rotor of wind energy unit w.
$c_{P,w}$	Power coefficient of wind energy unit w.
cc_{rt}^{k}	Scheduling cost of point k of offer package DRP r at time t.
$c_{\mathrm{curt},wts}$	Cost of 1-MWh wind power curtailment from wind generator w at time t.
DR	Ramp down limit.
ec_{rt}^{k}	Deployment cost of point k of scheduled offer by DRP r at time t.
l_{d}	Involuntary load shedding at load d.
MD_{i}	Minimum down time for unit i.
MU_{i}	Minimum up time for unit i.
p_{s}	Probability of scenario s of wind and load uncertainty.
$P_{D,d}$	Power demand at load d.
$P_{\max}$	Maximum power generation of unit i.
$P_{\min}$	Minimum power generation of unit i.
q_{r}^{k}	kth discrete DRR value of the bid of DRP r.
$\rho_{\mathrm{air},w}$	Air density at region where wind unit w is located.
$\rho_{\alpha,i}$	Capacity cost of reserve type α for unit i.
TD_{i0}	Number of hours unit i has been offline initially.
TU_{i0}	Number of hours unit i has been online initially.
$v_{\mathrm{CI},w}$	Cut-in wind speed of wind energy unit w.
$v_{\mathrm{CO},w}$	Cut-out wind speed of wind energy unit w.
$v_{R,w}$	Rated wind speed of wind energy unit w.
$VOLL_{d}$	Value of lost load at load d.
UR	Ramp up limit.
Δ_{s}	Allowed system load imbalance for the $N-1$ contingency in scenario s.

Abbreviations:

DR	Demand Response.
DRR	Demand Response Reserve.
DRP	Demand Response Provider.

I. INTRODUCTION

AS THE renewable energy integration in power systems evolves, the cost of supplying ancillary services becomes more prevalent with respect to operating decisions [1]. Wind energy is the fastest growing type of renewable energy due to its clean and indigenous nature. On the other hand, the installed wind capacity is not readily dispatchable due to its intermittent nature [2]–[7]. The effect of wind energy forecast errors is considered in the network-constrained market-clearing problem using a two-stage stochastic programming model in [8]. The first contribution of this paper is that it calculates the hourly reserves for addressing load and wind energy forecast errors in a stochastic framework while considering $N-1$ contingencies in power networks.

DR is a tariff that would encourage lower electricity consumptions [9]–[11]. DR can be motivated by either providing end-users with time-varying rates or giving incentives to such costumers to reduce loads at times when the electricity market price is high or the system reliability is at stake. The time-varying rates require an advanced measurement and communication infrastructure in order to convey real-time prices to end-use consumers, while the incentives are more suitable for a faster adaptation of electricity markets. DR provides financial incentives to customers who also benefit from lower hourly demands [12]–[16]. The second contribution of this paper would model the hourly DR in a discrete form in order to reflect the market behavior in an uncertain environment.

We propose a stochastic model in which wind and load forecast errors are addressed through Monte-Carlo-based scenarios in a two-stage stochastic programming model. The component outages are considered in an $N-1$ contingency model. To address the computation complexity, the problem is decomposed into a master problem to solve the UC and reserve schedules, and subproblems for considering the network security, for preselected $N-1$ contingencies, and load and wind forecast error scenarios. At the same time, DR is considered for managing hourly violations and reducing the cost of supplying the load. Load shedding is utilized whenever its contribution to lowering the stochastic cost is higher than that of allocating additional generating reserves. The proposed method would be used by an ISO or a vertical integrated utility to address the stochastic cost of security. The stochastic cost of security is defined as the difference between the scheduling cost of deterministic security-constrained unit commitment (SCUC) and that of considering uncertainties.

The rest of the paper is organized as follows. Mathematical models of DR and simulation of wind and load forecast error are discussed in Section II. The energy and A/S market clearing problem is introduced in Section III. Case studies are given in Section IV. Section V concludes this paper.

II. DR, Load, and Wind Energy Models

A. Demand Response Model

Demand response is formulated using a mixed-integer programming (MIP) formulation to fit the SCUC model. The bid should be in a discrete form since the demand response provider (DRP) represents an aggregated DR of end-users. Equations (1) and (2) in the following represent the scheduled demand response reserve (DRR) of DRP r at the time interval t and the related capacity cost. The value of q_r^0 would be greater than the minimum amount determined by the ISO. Equations (3) and (4) give the actual DRR utilized by DRP r in scenario s at time t, and the associated energy cost. A graphical representation of (1)–(5) is given in Fig. 1.

$$\mathrm{DRR}_{rt} = q_r^0 U_{rt}^0 + \sum_{k=1}^{NQ_r} \lambda_r^k U_{rt}^k \quad \forall r,\ \forall t \tag{1}$$

$$C_{\mathrm{DRR},rt} = cc_{rt}^0 q_r^0 U_{rt}^0 + \sum_{k=1}^{NQ_r} cc_{rt}^k \lambda_r^k U_{rt}^k \quad \forall r,\ \forall t \tag{2}$$

$$\mathrm{DRR}_{rts} = q_r^0 u_{rts}^0 + \sum_{k=1}^{NQ_r} \lambda_r^k u_{rts}^k \quad \forall r,\ \forall t,\ \forall s \tag{3}$$

$$C_{\mathrm{EDRR},rts} = ec_{rt}^0 q_r^0 u_{rts}^0 + \sum_{k=1}^{NQ_r} ec_{rt}^k \lambda_r^k u_{rts}^k \quad \forall r,\ \forall t,\ \forall s \tag{4}$$

$$\lambda_r^k = q_r^k - q_r^{k-1} \quad \forall r \tag{5}$$

In Fig. 1, "x" denotes a schedule k (i.e., $U_{rt}^0, U_{rt}^1, U_{rt}^2, U_{rt}^3 = 1$, and $U_{rt}^4 = 0$), and "+" denotes the discrete DR offer k deployed in scenario s (i.e., $u_{rts}^0, u_{rts}^1 = 1_t$ and $u_{rts}^2, u_{rts}^3, u_{rts}^4 = 0$).

B. Wind Energy and Load Simulation

This section discusses the modeling of forecast error scenarios for wind energy and system load which will be used in Monte Carlo simulations. The nonlinear wind speed to power conversion curve is given in (6), shown at the bottom of the page, and $P_{\psi,wts}$ is given as an input to the algorithm. The wind power generation w is subject to (7), shown at the bottom of the page. The auto-regressive moving average (ARMA)-based approach [17] provides scenarios for representing wind energy forecast errors. The wind energy forecast errors are simulated using ARMA series. The obtained ARMA series is sampled in order to obtain the forecast errors at each time step t in each scenario s. The corresponding available wind power is obtained via (6). The system load forecast error at time t is subject to a normal distribution $N(P_{Dt0}, \sigma^2)$, where P_{Dt0} is the forecasted system load at time t and σ is the load volatility. The system load distribution is sampled for scenario s at time t. The autocorrelation of the load forecast error model is assumed to be zero. The wind and load uncertainties are assumed independent.

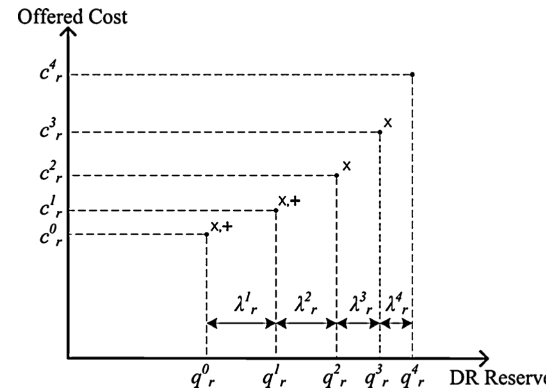

Fig. 1. Discrete DR bid scheduling and deployment.

III. Security-Constrained Wind Energy Scheduling

A. Objective Function

SCUC is modeled as an optimization problem for calculating the hourly unit commitment schedule at minimum production cost without compromising the system reliability. The regulation reserve is considered for following the short-term variations in the hourly customer demand or the scheduled generation, in order to maintain the system frequency within a permissible range. Spinning reserve is the unloaded generating capacity that can ramp up/down in 10 min. DR is assumed to be in the class of spinning reserves [1]. There are four terms in the SCUC objective function, as shown in (8), at the bottom of the next page.

The first term is composed of base case generation and reserve costs, and startup and shutdown costs. The second term is the capacity allocation cost corresponding to demand response. The third term is the cost of base case wind energy curtailment. The last term is the expected cost of deployment of regulation and spinning reserves, cost of deployment of DR reserves, cost of involuntary load shedding, and cost of wind curtailment for wind and load forecast scenarios. The scenarios $s = 1$ to *NC*

$$P_{\psi,wts}(\psi_{wts}) = \begin{cases} 0, & \text{if } \psi_{wts} < v_{\mathrm{CI},w} \\ 0.5 c_{p,w} \cdot \rho_{\mathrm{air},w} \cdot A_w \cdot (\psi_{wts})^3, & \text{if } v_{\mathrm{CI},w} \le \psi_{wts} < v_{R,w} \\ P_{R,w}, & \text{if } v_{R,w} \le \psi_{wts} < v_{\mathrm{CO},w} \\ 0, & \text{if } \psi_{wts} \ge v_{\mathrm{CO},w} \end{cases} \quad \forall w, \forall s \tag{6}$$

$$I_{wts} \cdot P_{\min,w} \le P_{wts} \le I_{wts} \cdot P_{\psi,wts}(\psi_{wts}) \quad \forall k, \forall s \tag{7}$$

represent $N-1$ contingencies and $s=NC+1$ to NS represent the wind and load forecast error scenarios.

We use a two-stage stochastic programming with recourse [18] in which the first stage variables are commitment states $(I_{,it})$, base case generations (P_{it0}, P_{wt0}), wind curtailments $(c_{\text{curt},wt0})$, and scheduled regulation and spinning reserves $(RR_{u,it}, RR_{d,it}, SR_{u,it}, SR_{d,it})$, and DRPs at hour t (DRR_{rt}). The second stage variables are scenario power generations $(P_{IMB,its}, P_{its}, P_{wts})$, deployed regulation and spinning reserves (RR_{its}, SR_{its}) and deployed DRPs (DRR_{rts}), wind curtailments $(c_{\text{curt},wts})$, and involuntary load shedding (l_{dts}) for scenario s and hour t.

The first stage variables are determined prior to the realization of uncertainties. The objective function is subject to the base case, $N-1$ contingencies, and wind and load forecast error scenario constraints in (9)–(20). The $N-1$ contingencies would only apply to the base case. The cost of deploying reserves for the $N-1$ contingencies is not considered in the objective function since the algorithm considers such contingencies as constraints and guarantees the scheduling of necessary generating reserves to respond to the $N-1$ contingencies without shedding any loads. Wind and load forecast errors are considered in scenarios ($s=NC+1$ to NS) for scheduling the hourly reserves.

B. Base Case Constraints

The power balance equation for the base case is given in (9). Load shedding is not allowed for the base case, since the available generation capacity would utilize the load.

$$\sum_{i=1}^{NG} P_{it0} + \sum_{i=1}^{NW} P_{wt0} = \sum_{d=1}^{ND} P_{D,dt0} \quad \forall t \tag{9}$$

Unit generation and reserve constraints and wind power curtailment

$$\begin{aligned}
&P_{it0} + RR_{u,it} + SR_{u,it} \le P_{\max,i} \cdot I_{it}\\
&P_{it0} - RR_{d,it} - SR_{d,it} \ge P_{\min,i} \cdot I_{it}\\
&0 \le RR_{u,it} \le RR_{\max,i}\\
&0 \le RR_{d,it} \le RR_{\max,i}\\
&0 \le SR_{u,it} \le SR_{\max,i}\\
&0 \le SR_{d,it} \le SR_{\max,i} \quad \forall i, \forall t\\
&0 \le \mathrm{DRR}_{rt} \le \mathrm{DRR}_{\max,r} \quad \forall r, \forall t\\
&0 \le P_{wt0} \le P_{\psi,wt0} \quad \forall w, \forall t\\
&P_{\text{curt},wt0} = P_{\psi,wt0} - P_{wt0} \quad \forall w, \forall t.
\end{aligned} \tag{10}$$

Ramp up and down limits

$$\begin{aligned}
&P_{it0} - P_{i(t-1)0} \le (1-y_{it})UR_i + y_{it}P_{\min,i}\\
&P_{i(t-1)0} - P_{it0} \le (1-z_{it})DR_i + z_{it}P_{\min,i}\\
&y_{it} - z_{it} = I_{it} - I_{i(t-1)}\\
&y_{it} + z_{it} \le 1 \quad \forall i,\ \forall t.
\end{aligned} \tag{11}$$

Minimum on/off time limits

$$\begin{aligned}
&UT_i = \max\{0, \min[NT, (MU_i - TU_{i0})I_{i0}]\}\\
&\sum_{t=1}^{UT_i}(1-I_{it}) = 0 \quad \forall i\\
&\sum_{m=t}^{t+MU_i-1} I_{im} \ge MU_i y_{it}\\
&\qquad\qquad \forall i,\ \forall t = UT_i+1,\ldots,NT-MU_i+1\\
&\sum_{m=t}^{NT}(I_{im} - y_{it}) \ge 0 \quad \forall i,\ \forall t = NT-MU_i+2,\ldots,NT\\
&DT_i = \max\{0, \min[NT, (MD_i - TD_{i0})(1-I_{i0})]\}
\end{aligned}$$

$$\min \sum_{t=1}^{NT}\left\{\begin{aligned}&\sum_{i=1}^{NG}\begin{bmatrix}F_{c,i}(P_{it0})\\ +F_{RR,i}(RR_{u,it}) + F_{RR,i}(RR_{d,it})\\ +F_{SR,i}(SR_{u,it}) + F_{SR,i}(SR_{d,it})\\ +SU_{it} + SD_{it}\end{bmatrix} + \sum_{r=1}^{NDR} C_{\mathrm{DRR},rt} + \sum_{w=1}^{NW} P_{\text{curt},wt0}\cdot c_{\text{curt},wt0}\\
&+\sum_{s=\mathrm{NC}+1}^{NS} p_s\left\{\begin{aligned}&\sum_{i=1}^{NG}(F_{c,i}(P_{its}) - F_{c,i}(P_{it0}))\\ &+\sum_{r=1}^{NDR} C_{\mathrm{EDRR},rts} + \sum_{d=1}^{ND} VOLL_d \cdot l_{dts}\\ &+\sum_{w=1}^{NW} P_{\text{curt},wts}\cdot c_{\text{curt},wts}\end{aligned}\right\}\end{aligned}\right\}. \tag{8}$$

$$\sum_{t=1}^{DT_i} I_{it} = 0 \quad \forall i$$
$$\sum_{m=t}^{t+MD_i-1} (1 - I_{im}) \geq MD_i z_{it}$$
$$\forall i, \forall t = DT_i + 1, \ldots, NT - MD_i + 1$$
$$\sum_{m=t}^{NT} (1 - I_{im} - z_{it}) \geq 0$$
$$\forall i,\ \forall t = NT - MD_i + 2, \ldots, NT. \quad (12)$$

Fuel and emission limits of thermal units can be added as in [19]. The generalized network constraints refer to network constraints in the base case and scenarios [20]

$$C_{\text{net}}(P_{it0}, P_{wt0}) \leq 0, \quad \forall t. \quad (13)$$

C. $N-1$ Contingency and Wind-Load Scenario Constraints

Here (14) and (15) indicate that the system load in scenario s is supplied by generation, reserves, DRRs, and involuntary load shedding

$$\sum_{i=1}^{NG} P_{its} + \sum_{r=1}^{NDR} \text{DRR}_{rts} + \sum_{d=1}^{ND} l_{dts} + \sum_{w=1}^{NW} P_{wts} = \sum_{d=1}^{ND} P_{D,dts}$$
$$\forall t,\ \forall s \quad (14)$$
$$P_{its} = P_{it0} + RR_{its} + SR_{its} \quad \forall i,\ \forall t,\ \forall s. \quad (15)$$

$P_{its} = 0$ for every t if generator i is on outage at scenario s. The deployed reserves and involuntary load shedding in scenario s are determined based on the scheduled generation capacities. The wind energy delivery in scenario s at time t is limited by the available wind generation

$$-RR_{d,it} \leq RR_{its} \leq RR_{u,it} \quad \forall i,\ \forall t,\ \forall s$$
$$-SR_{d,it} \leq SR_{its} \leq SR_{u,it} \quad \forall i,\ \forall t,\ \forall s$$
$$-\text{DRR}_{d,rt} \leq \text{DRR}_{rts} \leq \text{DRR}_{u,rt} \quad \forall r,\ \forall t, \forall s$$
$$0 \leq P_{wts} \leq P_{\psi,wts} \quad \forall w, \forall t, \forall s$$
$$P_{\text{curt},wts} = P_{\psi,wts} - P_{wts} \quad \forall w, \forall t, \forall s$$
$$0 \leq l_{dts} \leq l_{dt,\max} \quad \forall d, \forall t, \forall s$$
$$l_{dts} = 0 \quad \forall d, \forall t, s = \{1, \ldots, NC\}. \quad (16)$$

The involuntary load shedding variables are set to zero for the first iteration of $N-1$ contingency calculations so that consumers can utilize all available generation resources. However, if a few scenarios remain infeasible, the involuntary load shedding will be made available in the following iterations as an option for mitigating the scenario violations. The ramp limit for nonwind energy units in scenario s is

$$P_{its} - P_{i(t-1)s} \leq (1 - y_{it})UR_i + y_{it}P_{\min,i}$$
$$P_{i(t-1)s} - P_{its} \leq (1 - z_{it})DR_i + z_{it}P_{\min,i} \quad \forall i,\ \forall t,\ \forall s. \quad (17)$$

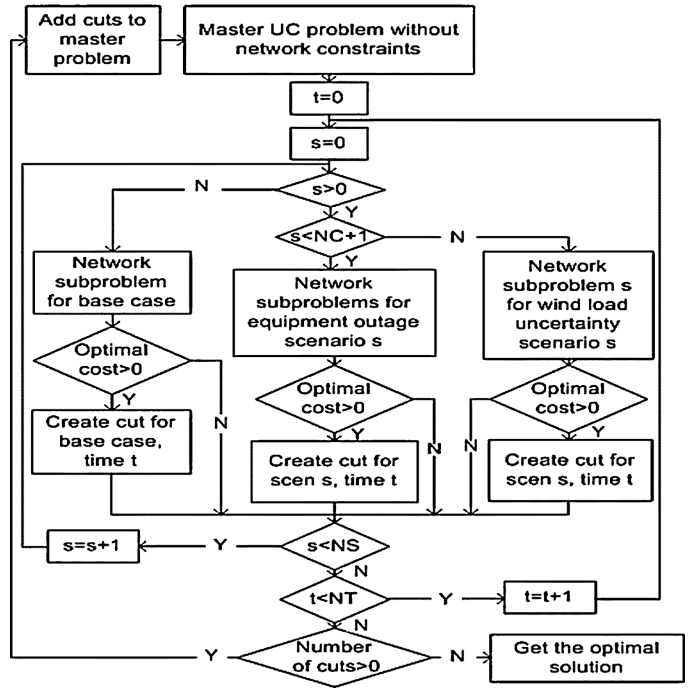

Fig. 2. Flowchart of the proposed scheduling algorithm.

Once a contingency occurs, the system load is defined in (18) as the total load minus the allowable system load imbalance Δ. The amount of system load imbalance is defined by the type of the contingency for an acceptable range of frequency changes [21]. The regulation reserve is considered in (18) and (19) for supplying the load in contingencies

$$\sum_{i=1}^{NG} P_{IMB,its} + \sum_{r=1}^{NDR} \text{DRR}_{rts} + \sum_{w=1}^{NW} P_{wts} \geq \sum_{d=1}^{ND} P_{D,dts} - \Delta_s$$
$$\forall s \in \{1, \ldots, NC\}, \forall t \quad (18)$$
$$P_{IMB,its} = P_{it0} + RR_{its} \quad \forall i, \forall s \in \{1, \ldots, NC\}, \forall t. \quad (19)$$

The network constraints in scenario s are represented by

$$C_{\text{net}}(P_{its}, P_{wts}, RR_{its}, SR_{its}, \text{DRR}_{rts}, l_{dts}) \leq 0 \quad \forall t, \forall s. \quad (20)$$

If there is a line outage in scenario s, (20) will incorporate the required changes in generator and load incidence matrices and the corresponding line flows [22].

IV. Proposed Solution Methodology

The proposed MIP problem is represented by the objective function (8), subject to constraints (9)–(20). For large systems with many possible contingencies and wind and load forecast errors, the problem might be intractable due to the increased size of constraints and variables. Therefore, we resort to decomposition as shown in Fig. 2. The algorithm depicts the application of Benders decomposition to the solution of the proposed scheduling problem.

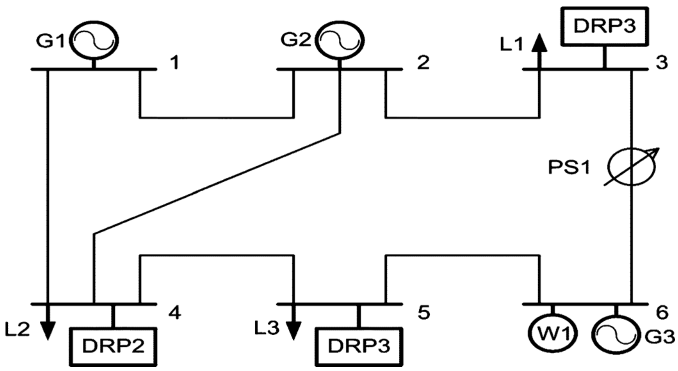

Fig. 3. One-line diagram for six-bus system.

The master UC problem includes first- and second-stage variables described in Section III-A plus the network cuts (21) for the base case and scenarios

$$C_{\mathrm{net}}(P_{it0}, P_{wt0}) \leq 0 \quad \forall t$$
$$C_{\mathrm{net}}(P_{its}, P_{wts}, RR_{its}, SR_{its}, \mathrm{DRR}_{rts}, l_{dts}) \leq 0 \quad \forall t, \forall s. \tag{21}$$

The dc power network subproblems consider the master problem solution to detect flow violations and send cuts to the master UC problem as necessary [20].

V. Case Studies

The proposed algorithm is applied to a six-bus system to capture the essential characteristics of the algorithm, and to the modified IEEE-118 bus system to assess the performance of the proposed solution. The method is also applied to the northwest region of the Turkish electric power market.

A. Six-Bus System

The six-bus system data are given in [3] in which a wind energy unit with a maximum power output of 20 MW is added at bus 6. The one-line diagram of the system is given in Fig. 3. The system has three thermal units, four transmission lines, two tap-changing transformers, and one phase shifter for MW control. The generation units from cheapest to most expensive are G1, G2, and G3. The regulation reserve prices are 14, 13, and 11 \$/MW, spinning reserve prices are 11, 10, and 8 \$/MW for three units, respectively. Flow limits of lines are 200, 150, 150, 100 MW for lines 1–2, 1–4, 2–4, 5–6, respectively.

DRP bids include three discrete points with q_r^k of 1.8, 3.6, and 5.4 MW, and cc_{rt}^k of 10, 13, and 16 \$/MW, respectively, at each time interval. The deployment cost ec_{rt}^k is 10 \$/MW and the *VOLL* is 450 \$/MWh at each load bus. The scenario reduction tool of the General Algebraic Modeling System (GAMS) is used in which the reduction method is set to the Mix of Fast Backward/Forward methods [23]. Initially there were 1500 Monte Carlo scenarios with even probabilities (1/1500) which are reduced to 10 scenarios with a relative distance of 75%. The relative distance would be 70% and 83% when the Monte Carlo scenarios are reduced to 50 and 9 scenarios, respectively [24].

The wind curtailment cost is 50 \$/MW which is higher than the largest marginal cost of the given thermal units. The standard deviation of wind forecast error will gradually increase from 0% to 6.5% of the forecast from $t = 0$ to 24. The standard deviation of the system load forecast error is 3% of the load forecast at each time interval. The probability of scenarios is given in Table I. The forecasted wind and its error scenarios are depicted in Fig. 4. The following three case studies are considered:

Case 1) Deterministic case (without network contingencies).
Case 2) Stochastic wind and load forecast errors in Case 1.
Case 3) $N-1$ contingencies in Case 2.

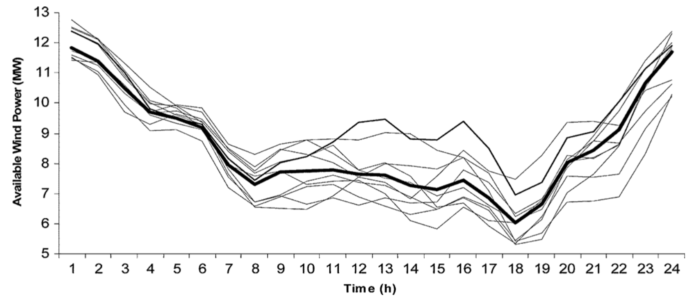

Fig. 4. Wind power forecast and scenarios.

TABLE I
PROBABILITY OF SCENARIOS AFTER SCENARIO REDUCTION

Scenario	1	2	3	4	5
Probability	0.26	0.12	0.08	0.07	0.14
Scenario	6	7	8	9	10
Probability	0.09	0.02	0.07	0.07	0.08

Case 1: This case provides a reference in which no contingency or uncertainty is considered. The total system operation cost is \$99 061. Table II depicts the scheduling of three thermal units and the wind energy units. The available wind energy is fully utilized since the wind energy units are assumed to be price-takers. G1 is scheduled at all hours since it is the cheapest unit. G2 is committed in the first hour due to min up constraints. G2 is scheduled to generate between hours 11–21, while G3 is scheduled between 13–19, since these are the next expensive units in the ascending order. No reserves or DR are scheduled in the base case.

Case 2: This case includes wind and load forecast errors which are considered through the Monte Carlo scenarios. The total system cost increases to \$104 431. The base case dispatch is identical to that of Case 1. Fig. 5 depicts the wind power curtailments in the base case and scenarios. The algorithm curtails small amounts of wind in order to not utilize expensive regulation and spinning-down reserves. However, it should be noted that wind power curtailment might not be allowed in certain cases. The algorithm does not schedule regulation reserves in Case 2 other than 1.12 MW for hour 12 and 2 MW for hour 19 from G3. The spinning reserve dispatch and DR are given in Table III. These are the maximum deployable reserves available to the scenarios. Involuntary load shedding of 790, 50, 1450, 470, 120, and 7010 kWh is utilized in scenarios 1, 2, 3, 4, 5, and 7, respectively. The maximum load shedding occurs in the seventh scenario with the smallest probability. The expected system cost in Case 2 will increase to \$104 592 when the involuntary load shedding is not allowed. The day-ahead system cost without DRR is \$104 973 which will be reduced once DRR replaces the expensive units.

Case 3: Two $N-1$ contingencies of G3 and the transmission line (between buses 3–6) are considered along with the

TABLE II
CASE 1 GENERATION DISPATCH (MW)

Hour	G1	G2	G3	W1
1	161.88	10	0	11.82
2	162.05	0	0	11.4
3	156.33	0	0	10.51
4	153.13	0	0	9.7
5	153.67	0	0	9.49
6	159.51	0	0	9.18
7	173.91	0	0	7.95
8	191.92	0	0	7.3
9	206.97	0	0	7.7
10	218.79	0	0	7.75
11	230	0	0.4	7.79
12	230	0	8.16	7.66
13	230	10	4.42	7.61
14	230	10	6.19	7.28
15	230	11.71	10	7.12
16	230	18.47	10	7.43
17	230	19.27	10	6.85
18	230	10.64	10	6.04
19	230	10	9.25	6.64
20	230	0	9.08	8.02
21	230	0	8.61	8.44
22	227.57	0	0	9.11
23	199.39	0	0	10.68
24	194	0	0	11.68

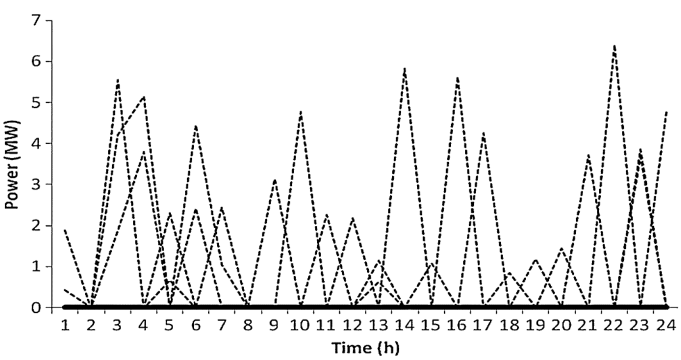

Fig. 5. Wind generation curtailments in Case II. Solid line: zero curtailment at base case. Dotted line: wind energy curtailments in scenarios.

TABLE III
CASE 2 RESERVE DISPATCH (MW)

Hour	SR_u			SR_d			DR		
	G1	G2	G3	G1	G2	G3	DRP1	DRP2	DRP3
1	5.07	0	0	4.83	0	0	0	0	0
2	8.55	0	0	7.04	0	0	0	0	0
3	5.38	0	0	2.29	0	0	0	0	0
4	5.77	0	0	2.21	0	0	0	0	0
5	7.87	0	0	2.28	0	0	0	0	0
6	4.51	0	0	0.88	0	0	0	0	0
7	10.82	0	0	4.81	0	0	0	0	0
8	4.12	0	0	4.56	0	0	0	0	0
9	7.98	0	0	4.36	0	0	0	0	0
10	4.66	0	0	2.35	0	0	0	0	0
11	1.51	0	6.67	2.73	0	1.9	0	0	0
12	0	0	1.67	0	0	6.67	1.8	1.8	1.8
13	0	0	5.43	0	0	4.42	0	0	1.8
14	0	2.32	6.67	0	2.85	0.32	0	0	0
15	0	6.06	1.05	0	2.76	6.67	0	0	0
16	0	7.59	0.02	0	8.5	0	0	0	0
17	0	12.31	0	0	3.06	0	0	0	0
18	0	8.41	0	0	0.64	3.4	0	0	0
19	0	0	0.75	0	0	6.67	3.6	3.6	3.6
20	0	0	0.92	0	0	6.67	0	0	1.8
21	0	0	1.39	0	0	6.67	5.4	5.4	5.4
22	3.34	0	6.67	0	0	2.37	0	0	0
23	13.83	0	0	3.98	0	0	0	0	0
24	4.34	0	0	6.63	0	0	0	0	0

TABLE IV
CASE 3 RESERVE DISPATCH (MW)

Hour	RR_u		SR_u			SR_d		
	G2	G3	G1	G2	G3	G1	G2	G3
1	0	0	5.07	0	0	4.83	0	0
2	0	0	8.55	0	0	7.04	0	0
3	0	0	5.38	0	0	2.29	0	0
4	0	0	5.77	0	0	2.21	0	0
5	0	0	7.87	0	0	2.28	0	0
6	0	0	4.51	0	0	0.88	0	0
7	0	0	10.82	0	0	4.81	0	0
8	0	0	4.12	0	0	4.56	0	0
9	0	0	7.98	0	0	4.36	0	0
10	0	0	4.66	0	0	2.35	0	0
11	0	0	8.17	0	0	4.63	0	0
12	0	0	1.84	4.83	0	7.78	0	0
13	3.33	0	0	0	6.67	3.95	1.08	0.01
14	3.32	0	0	0	6.67	3.8	2.87	0
15	8.05	0	0	0	1.95	6.85	3.66	0
16	10	0	0	0	0	6.79	8.47	0
17	10	0	0.35	1.96	0	7.32	0	0
18	9.78	0	0	0	0.22	4.02	0.86	0
19	3.33	0	0	0	6.67	3.54	5.92	0
20	0	0	0	0	3.56	6.23	0	0
21	0	3.02	1.39	0	6.67	6.7	0	0
22	0	0	2.43	0	0	2.37	0	0
23	0	0	13.83	0	0	3.98	0	0
24	0	0	4.34	0	0	6.63	0	0

10 wind and load forecast scenarios. The system cost increases to \$105 848 in Case 3 with an expected involuntary load shedding of 138.2 kWh. The involuntary load shedding in this case is due to infeasibilities in wind and load scenarios. The DR schedule is identical to that in Case 2. The reserve dispatch for Case 3 is given in Table IV. The expensive regulation reserve is deployed for managing contingencies. The wind generation in the base Case 3 is curtailed, similar to that in Case 2, to consider the $N-1$ contingencies. When DRR is not allowed, the optimal expected system cost is \$106 041 with an expected involuntary load shedding of 20 kWh.

Sensitivity Analysis: A sensitivity analysis is performed to evaluate the effect of wind and load forecast errors. Fig. 6 depicts the error levels versus the expected costs. In order to compare the effect of wind and load forecast errors, the standard deviation of wind is normalized by the maximum capacity of wind energy unit and the standard deviation of load is normalized by the maximum system load. First the system load forecast error is fixed to that of Case 3 (3%) and wind forecast error is varied starting from that of Case 3 (6.5%) to 32%. We observe that the wind forecast error does not affect the expected system cost significantly due to the limited availability of wind generation. Then the wind forecast error is fixed to that of Case 3 (6.5%) and the system load forecast error is varied starting from that of Case 3 (3%) to 12%. The expected system cost increases sharply due to the allocation and the deployment of additional reserves to respond to the increasing volatility of the system load.

Fig. 7 depicts the expected cost of uncertainty at each wind penetration level when the standard deviation of system load

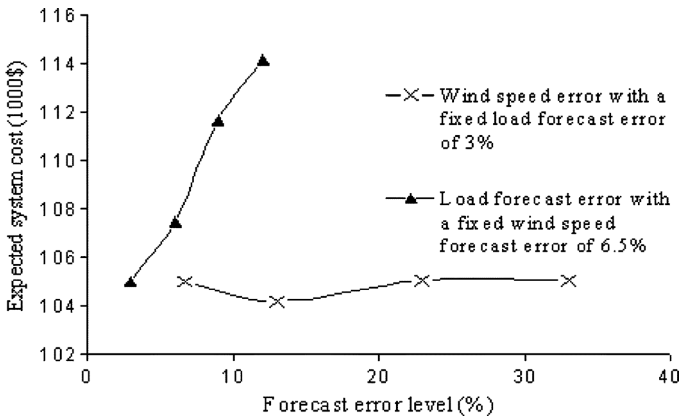

Fig. 6. Expected system cost versus wind energy and load forecast errors.

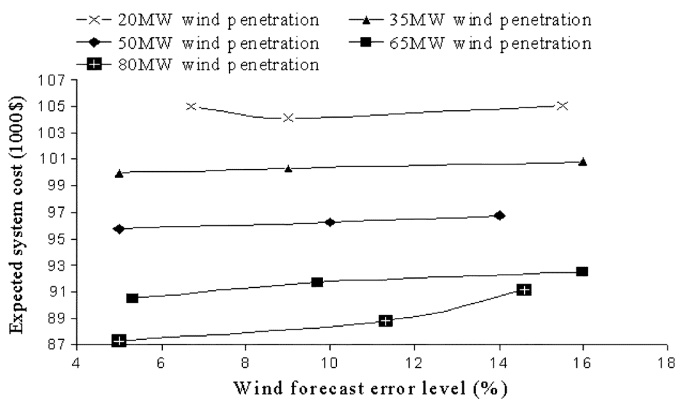

Fig. 7. Expected system cost with the wind penetration level.

TABLE V
RESERVE ALLOCATION AMONG UNITS IN THE 118-BUS SYSTEM CASE

	Regulation Up	Spinning Up	Spinning Down
Considering Demand Response	-	7, 29, 34, 39, 43, 45, 47, 51	5, 7, 10, 19, 22, 26, 27, 29, 30, 34, 39, 40, 43, 45, 47, 51, 52
No Demand Response	4, 7, 19, 22, 23, 26, 28, 30, 40	7, 10, 11, 14, 19, 22, 26, 27, 29, 30, 34, 35, 36, 37, 39, 40, 43, 45, 47, 48, 51, 52, 53	7, 10, 19, 22, 26, 27, 29, 30, 34, 36, 39, 40, 43, 45, 47, 48, 51, 52

forecast error is 3%. The wind penetration refers to the installed capacity, and the hourly mean production is proportional to the installed capacity. Here, for a lower wind penetration, the sensitivity of the expected system cost to wind energy forecast error is insignificant. This is because the required reserve would be low as the uncertainty is increased at the limited penetration level of 20 MW. However, the expected cost would increase for a higher penetration level as the forecast error is increased.

B. Modified IEEE 118-Bus System

The Modified IEEE 118-Bus system is used to evaluate the efficiency of the proposed method. There are 186 branches and 91 loads. Three wind energy units are added to the 54 existing units. There are 50 DRPs at certain load buses which provide bids to the reserve market. The VOLL is 400 $/MWh at each load bus. Seven $N-1$ contingencies include the outage of generators at buses 77, 82, 105, 113 and the outage of lines 17–113, 114–115, and 17–113. The wind and load forecast errors are represented by 1500 Monte Carlo scenarios. The number of scenarios is reduced to 12 by using forward–backwards scenario

TABLE VI
SCALABILITY ANALYSIS

N-1 Contingencies	Uncertainty Scenarios	Variables	Equality Constraints	Inequality Constraints
3	12	422,640	111,552	146,088
	18	583,488	157,776	199,944
	24	744,336	204,000	253,800
3	12	422,640	111,552	146,088
7		519,504	131,856	181,800
11		616,368	152,160	217,512

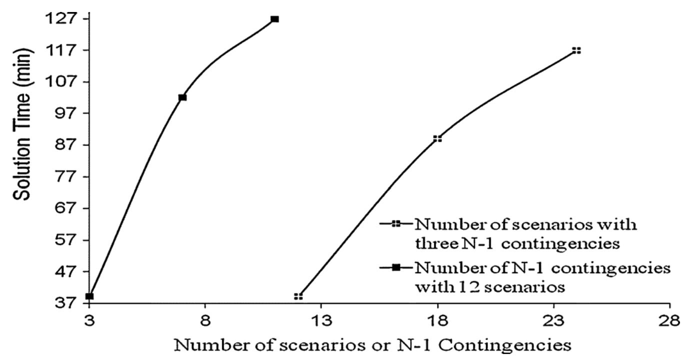

Fig. 8. Solution time versus $N-1$ contingency or uncertainty scenarios.

reduction techniques [23]. The data are available at motor.ece.iit.edu/data/Data_118_Bus.pdf. Table V shows the generation units with allocated reserves, $RR_{u,it}, RR_{d,it}, SR_{u,it}, SR_{d,it}$. Here, the $RR_{u,it}, RR_{d,it}, SR_{u,it}, SR_{d,it}$ values for the listed units are positive for at least one hour in 24 hours.

The total expected system cost is $1 270 517 without DR. The allocated reserves include 155 MWh of regulation-up, 3076 MWh of spinning-up, and 2204 MWh of spinning-down reserve. No involuntary load shedding is deployed. When DR is considered, the expected cost reduces to $1 263 126, and expensive regulation reserve capacity is not allocated. The spinning-up reserve is reduced to 251 MWh while the spinning-down reserve remains nearly the same at 2376 MWh. 2987 MWh of DR is allocated using DRPs for contingency and wind and load forecast error scenarios whenever they are cheaper than spinning-up reserve bids. Similar to the case without DR, no involuntary load shedding is allocated. The solution curtailed 182.27 MWh of wind energy for accommodating $N-1$ contingencies and forecast errors in both cases. The solution time in the latter case is 1 hour, 42 minutes, with an Intel Xeon 2.4 GHz CPU and 64 GB of RAM.

Scalability Analysis: This analysis evaluates the performance when the number of $N-1$ contingencies and the error forecast uncertainty are increased. Here, two tests are performed. First, three $N-1$ contingencies are considered with 12, 18, and 24 forecast error scenarios. The change in the solution time is observed. Second, $N-1$ contingencies are changed to 3, 7, and 11 while the number of forecast error scenarios is kept at 12. The results are presented in Table VI and Fig. 8. Here, the slope of the solution time is decreased as the number of contingencies and the level of uncertainties are increased. This is because some scenarios would require higher reserve allocations, and once the situation with these scenarios is resolved, the additional scenarios might not require much further reserve allocations. Besides, the performance is more sensitive to the number

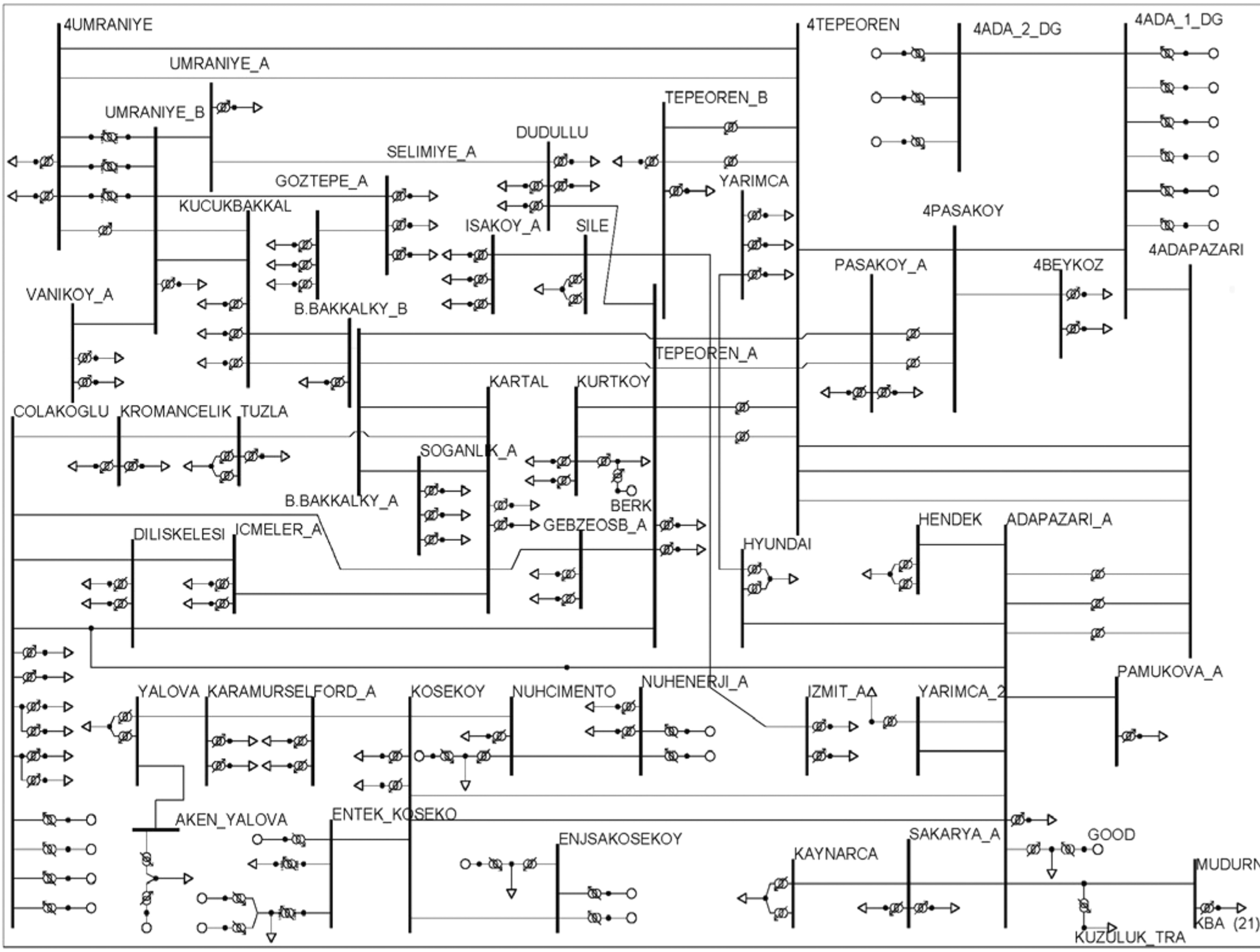

Fig. 9. Northwest region of Turkish Electric Power Network.

of $N-1$ contingencies since one contingency could introduce more constraints to the problem.

C. Northwest Region of Turkish Power System

Turkey has taken major steps towards building the country's electricity market since the enactment of Turkish Electricity Market Law in 2001 [25]. In this section, the proposed model is applied to the northwest region of the Turkish Power System which includes large industrial activities. The proposed scheduling model would study the coordination of hourly reserve and DR requirements when wind and load forecast uncertainties are considered. The subsystem depicted in Fig. 9 is composed of 173 buses, 28 thermal generating units, 66 branches, and 131 transformers.

Two $N-1$ contingencies are considered as the outages of one of the generators at bus NUHENERJI_A and the transmission line COLAKOGLU-KROMANCELIK. 1500 scenarios are created to simulate wind and load forecast errors which are reduced to 12 scenarios. The standard deviations for wind and load forecaster error are 6.5% and 4%, respectively. Considerable industrial loads appear at buses DILISKELESI, COLAKOGLU, ICMELER, DUDULLU, and GEBZEOSB. These loads are mostly composed of shipyards, steel mills, and cement manufacturing facilities in an industrial zone.

Three 100-MW wind farms are located at three buses SILE, KARAMURSEL, and YALOVA, which have considerable wind potential. Detailed data are included in motor.ece.iit.edu/data/Data_TR.pdf. Six DRP buses are DILISKELESI, COLAKOGLU, DUDULLU, KOSEKOY, KUCUKBAKKAL, and GEBZEOSB, with both residential and industrial loads. For instance, cement factories could curtail consumption and shift production when required by the ISO. The DRP bids are 7, 14, and 21 MW at 7, 9, and 11 \$/MW and the deployment prices at 17.5, 22.5, and 27.5 \$/MW, respectively.

The expected day-ahead system cost without DRR is \$559 039 while the cost reduces to \$549 289 when DRR is considered. The wind curtailment is 78.38 MWh in both cases (see Table VII). DRR replaces 870 MWh of spinning-up, 915 MWh of spinning-down, and 44 MWh of regulation-up reserves, and reduces the costs by \$9750. The DRPs are paid a total of \$17 045, for participating in the DRR program.

VI. Conclusion

The proposed method is used to analyze the effect of $N-1$ contingencies, wind and load uncertainties, and DRP bids in the hourly generation scheduling. The proposed algorithm curtails

TABLE VII
ALLOCATED DRRs (MW) OF DRPs

Hour		1	2	3	4	5	6	7	8	9	10	11	12
DRP	1	7	0	0	0	7	7	7	7	7	7	7	7
	2	7	0	7	0	0	0	0	14	7	7	7	7
	3	0	7	7	0	0	0	7	14	14	0	14	14
	4	7	7	0	0	7	0	0	7	7	7	7	7
	5	0	7	7	0	0	0	0	14	7	7	7	7
	6	7	0	7	0	0	7	7	14	7	7	7	7
Hour		**13**	**14**	**15**	**16**	**17**	**18**	**19**	**20**	**21**	**22**	**23**	**24**
DRP	1	7	0	7	7	7	7	7	14	21	0	7	0
	2	7	7	7	7	7	7	7	14	14	7	7	0
	3	14	14	14	14	14	14	14	14	14	7	14	14
	4	7	7	7	7	7	7	7	0	0	0	7	0
	5	7	7	7	7	7	7	7	7	7	7	7	7
	6	7	7	7	7	7	7	7	14	14	7	7	0

the wind generation in scenarios in order to not allocate expensive regulation and spinning-down reserves. The sensitivity analyses show that the expected system cost is more sensitive to load forecast errors. The effect of wind forecast error depends on the wind penetration level. The system cost decreases as the wind penetration increases since the operating cost of wind energy units is neglected. However, the expected cost increases considerably with the increasing wind forecast errors. A scalability analysis is performed which shows that the rate of change in the solution time decreases sharply as the number of considered contingencies is increased or wind and load volatilities are higher. Furthermore, it is observed that the solution performance is more sensitive to the number of contingencies since contingencies could add more variables and constraints to the problem. It is also shown that the integration of DR at proper locations and periods would reduce the cost of the security-based power system scheduling.

REFERENCES

[1] M. Shahidehpour, H. Yamin, and Z. Y. Li, *Market Operations in Electric Power Systems*. New York: Wiley, 2002.

[2] Global Wind 2008 Report, GWEC, Global Wind Energy Council, Brussels, Belgium [Online]. Available: http://www.gwec.net

[3] J. Wang, M. Shahidehpour, and Z. Li, “Security-constrained unit commitment with volatile wind power generation,” *IEEE Trans. Power Syst.*, vol. 23, no. 4, pp. 1319–1327, Aug. 2008.

[4] E. D. Castronuovo and J. A. Pecas-Lopes, “On the optimization of the daily operation of a wind-hydro power plant,” *IEEE Trans. Power Syst.*, vol. 19, no. 3, pp. 1599–1606, Aug. 2004.

[5] B. C. Ummels, M. Gibescu, E. Pelgrum, W. L. Kling, and A. J. Brand, “Impacts of wind power on thermal generation unit commitment and dispatch,” *IEEE Trans. Energy Convers.*, vol. 22, no. 1, pp. 44–51, Mar. 2007.

[6] Y. V. Makarov, C. Loutan, J. Ma, and P. de Mello, “Operational impacts of wind generation on California power systems,” *IEEE Trans. Power Syst.*, vol. 24, no. 2, pp. 1039–1050, May 2009.

[7] A. Fabbri, T. Gomez San Roman, J. Rivier Abbad, and V. H. M. Quezada, “Assessment of the cost associated with wind generation prediction errors in a liberalized electricity market,” *IEEE Trans. Power Syst.*, vol. 20, no. 3, pp. 1440–1446, Aug. 2005.

[8] J. M. Morales, A. J. Conejo, and J. Pérez-Ruiz, “Economic valuation of reserves in power systems with high penetration of wind power,” *IEEE Trans. Power Syst.*, vol. 24, no. 2, pp. 900–911, May 2009.

[9] U.S. Department of Energy, Benefits of demand response in electricity markets and recommendations for achieving them Feb. 2006.

[10] F. Boshell and O. P. Veloza, “Review of developed demand side management programs including different concepts and their results,” in *Proc. IEEE/PES Transmission and Distribution Conf. Exposition: Latin America*, Seattle, WA, 2008, pp. 1–2.

[11] F. Rahimi, “Overview of demand response programs at different ISOs/RTOs,” in *Proc. IEEE/PES Power Systems Conf. Exposition*, Bogota, Colombia, 2009, pp. 1–7.

[12] M. Parvania and M. Fotuhi-Firuzabad, “Demand response scheduling by stochastic SCUC,” *IEEE Trans. Smart Grid*, vol. 1, no. 1, pp. 89–98, Jun. 2010.

[13] W. Uturbey and A. S. Costa, “Dynamic optimal power flow approach to account for consumer response in short term hydrothermal coordination studies,” *IET Gener. Transm. Distrib.*, vol. 1, no. 3, pp. 414–421, May 2007.

[14] D. Mennit, F. Costanzo, N. Scordino, and N. Sorrentino, “Purchase-bidding strategies of an energy coalition with demand-response capabilities,” *IEEE Trans. Power Syst.*, vol. 24, no. 3, pp. 1241–1255, Aug. 2009.

[15] C.-L. Su and D. Kirschen, “Quantifying the effect of demand response on electricity markets,” *IEEE Trans. Power Syst.*, vol. 24, no. 3, pp. 1199–1207, Aug. 2009.

[16] Q. Zhang and X. Wang, “Quantifying hedge contract characterization and risk-constrained electricity procurement,” *IEEE Trans. Power Syst.*, vol. 24, no. 3, pp. 1547–1558, Aug. 2009.

[17] L. Soder, “Simulation of wind speed forecast errors for operation planning of multiarea power systems,” in *2004 Int. Conf. Proc. Probabilistic Methods Applied to Power Systems*, Sep. 12–16, 2004, pp. 723–728.

[18] J. R. Birge and F. Louveaux, *Introduction to Stochastic Programming*. New York: Springer, 1997.

[19] Y. Fu, M. Shahidehpour, and Z. Li, “AC contingency dispatch based on security-constrained unit commitment,” *IEEE Trans. Power Syst.*, vol. 21, no. 2, pp. 897–908, May 2006.

[20] M. Shahidehpour and Y. Fu, “Benders decomposition: Applying Benders decomposition to power systems,” *IEEE Power Energy Mag.*, vol. 3, no. 2, p. 20, Mar. 2005.

[21] A. Wood and B. Wollenberg, *Power Generation Operation and Control*, 2nd ed. New York: Wiley, 1996.

[22] J. Wang, M. Shahidehpour, and Z. Li, “Contingency-constrained reserve requirements in joint energy and ancillary services auction,” *IEEE Trans. Power Syst.*, vol. 24, no. 3, pp. 1457–1468, Aug. 2009.

[23] GAMS Development Corporation, GAMS—The Solver Manuals Washington, DC [Online]. Available: www.gams.com/

[24] H. Heitsch and W. Romisch, “Scenario reduction algorithms in stochastic programming,” *Computat. Optimizat. Applicat.*, vol. 24, no. 2–3, pp. 187–206, Feb./Mar. 2003.

[25] C. Sahin and M. Shahidehpour, “Interdependence of NG and electricity infrastructures in Turkey,” in *Proc. 2009 IEEE PES General Meeting*, Calgary, Canada.

Cem Sahin (M’11) received the M.S. and Ph.D. degrees in electrical engineering from Middle East Technical University (METU), Turkey, in 2003 and 2010, respectively.

He was a visiting scientist in the Robert W. Galvin Center for Electricity Innovation, Illinois Institute of Technology, in 2009. His research interests include power systems optimization, wind energy integration, and power markets.

Mohammad Shahidehpour (S’79–M’81–SM’86–F’01) is the Bodine Chair Professor and Director of Robert W. Galvin Center for Electricity Innovation, Illinois Institute of Technology. He is a Research Professor at the King Abdulaziz University, Saudi Arabia, and Honorary Professor at Sharif University of Technology, Iran, and North China Electric Power University, China.

Ismet Erkmen is the Chairman in the Electrical and Computer Engineering Department, Middle East Technical University (METU), Ankara, Turkey. His research interests are control of large-scale systems and power systems optimization.